EVALUATION OF THE PLASTIC CRITICAL DEPTH IN SEISMIC ACTIVE LATERAL EARTH PRESSURE PROBLEMS USING THE STRESS-CHARACTERISTICS METHOD

Amin Keshavarz
Persian Gulf University,
School of Engineering
Shahid Mahini Street, Bushehr, Iran
E-mail: keshavarz@pgu.ac.ir

Keywords

plastic critical depth, stress characteristics, active lateral earth pressure, seismic

Abstract

The plastic critical depth or the conventional tension crack depth has a considerable effect on the active lateral earth pressure in cohesive soils. In this paper the depth for c-ϕ soils has been evaluated in the seismic case using the stress-characteristics or slip-line method. The plastic critical depth was calculated on the basis of the theory of the stress-characteristics method and by considering the horizontal and vertical pseudo-static earthquake coefficients. The proposed solution considers the line of discontinuity in the stress-characteristics network. The earth slope, wall slope, cohesion and friction angle of the soil and the adhesion and the friction angle of the soil-wall interface were considered in the analysis as well. The results show that the plastic critical depths of this study are smaller than those of the other methods and are closer to the modified Mononobe-Okabe method. The effects of the wall and the backfill geometry, the mechanical properties of the soil and the pseudo-static coefficients were studied.

1 INTRODUCTION

In cohesive soils, the computed active lateral earth pressure can be negative from the ground surface to some depth. The plastic critical depth is the depth where the computed soil pressure is negative from the ground surface to that depth. To calculate the active lateral earth pressure many engineers assume that the lateral earth pressure is zero from the ground surface to the plastic critical depth. Therefore, the calculation of the plastic critical depth is important in any evaluation of the active lateral earth pressure. Numerical examples showed that if the plastic critical depth is considered, the static lateral earth pressure can be more than 20 to 40 percent of the lateral earth pressure, without taking into account the plastic critical depth [1].

Peng [2] assumed that the failure surface is planar and evaluated the static active lateral earth pressure using the limit-equilibrium method. He considered the plastic critical depth and the surcharge in his study. Peng [3] modified the Mononobe-Okabe method to calculate the seismic active lateral earth pressure. He presented some equations to calculate the lateral earth pressure and the plastic critical depth in *c-ϕ* soils.

Nian and Han [4] calculated the seismic active lateral earth pressure against rigid retaining walls. They used the Rankin theory and proposed an equation to estimate the plastic critical depth. In their study the retaining wall is vertical, but the ground surface can be inclined. Also, Iskander et al. [5] expanded the Rankin solution for seismic cases and proposed an equation for the plastic criti-

cal depth. Ma et al. [6] evaluated the lateral earth pressure and the plastic critical depth using the pseudo-dynamic method. Recently, Lin et al. [7] used the slice-analysis method to compute the nonlinear distribution of the seismic active earth pressure of cohesive-frictional soil.

The stress-characteristics or slip-line method is one of the famous methods for analysing geotechnical problems. This method was presented by Sokolovski [8, 9]. Reece and Hettiaratchi [10] and Kumar and Chitikela [11] used the stress-characteristics method to compute the passive lateral earth pressure. Cheng [12] proposed a rotation of the axes in the stress-characteristics method to determine the seismic lateral earth pressure. Peng and Chen [13] applied this method to compute the active lateral earth pressure in the static case. The stress-characteristics method has also been used to evaluate the stability of reinforced soil structures [14, 15].

Table 1 summarizes the different methods for calculating the plastic critical depth. The parameters used in the table will be defined in the next sections. It is clear that most of the methods proposed closed-form solutions. Some of them need trial and error, and three of them consider all the parameters in the solution.

In this paper the plastic critical depth is studied using the stress-characteristics method. Although Peng and Chen [13] used this method to compute the active lateral earth pressure, they did not consider the seismic effects

Table 1. Summary of different methods to calculate the plastic critical depth.

No.	Proposed by	Theory	Parameters considered				Comments
1	Rankin	Simple Rankin	c_w	☒	δ_w	☒	- The simplest equation (Eq. (25))
			θ	☒	β	☒	
			k_h	☒	k_v	☒	
			q	☑			
2	Peng, 2012 [3]	Modified Mononobe-Okabe	c_w	☑	δ_w	☑	- Closed form without trial and error
			θ	☑	β	☑	
			k_h	☑	k_v	☑	
			q	☑			
3	Ma et al., 2012 [6]	Pseudo-dynamic	c_w	☑	δ_w	☑	-No closed form - Needs optimization
			θ	☑	β	☒	
			k_h	☑	k_v	☑	
			q	☑			
4	Peng and Chen, 2013 [13]	Slip line	c_w	☑	δ_w	☑	-Closed form -Needs trial and error -When β=0 solution can be found without trial and error
			θ	☑	β	☑	
			k_h	☒	k_v	☒	
			q	☑			
5	Iskandet et al., 2013 [5]	Expanded Rankin	c_w	☒	δ_w	☒	- Closed form without trial and error
			θ	☑	β	☑	
			k_h	☑	k_v	☑	
			q	☒			
6	Nian and Han, 2013 [4]	Modified Rankin	c_w	☒	δ_w	☒	- Closed form without trial and error
			θ	☒	β	☑	
			k_h	☑	k_v	☑	
			q	☒			
7	Lin et al., 2015 [7]	Slice analysis method	c_w	☑	δ_w	☑	-Closed form -Needs trial and error
			θ	☑	β	☑	
			k_h	☑	k_v	☑	
			q	☑			
8	This study	Slip line	c_w	☑	δ_w	☑	-Closed form -Needs trial and error -When β=k_h=k_v=0, solution can be found without trial and error
			θ	☑	β	☑	
			k_h	☑	k_v	☑	
			q	☑			

and the discontinuity line in the stress field. In this study, the estimation of the plastic critical depth is explained clearly, and several analyses are made in different cases.

2 THEORY

The backfill is a c-ϕ soil, where c and ϕ are the cohesion and the friction angle of the soil, respectively. The soil obeys the Mohr-Coulomb failure criterion. The retaining wall is rigid, and the soil-wall interface has the adhesion c_w and the friction angle δ_w.

Figure 1 shows a soil element in the plane-strain case. There are two families of failure orientations, PA and PB, known as the negative and positive characteristics, and make a stress field. As shown, the stress-characteristics lines make the angle $\mu = \pi/4 - \phi/2$ with the orientation of the principal stress σ_1 [9]. Each point in the soil media has four features, x, z, p and ψ, where x and z are the coordinates of the point and p is the average stress in the Mohr's circle and ψ is the angle between σ_1 and the horizontal axis (Figure 1).

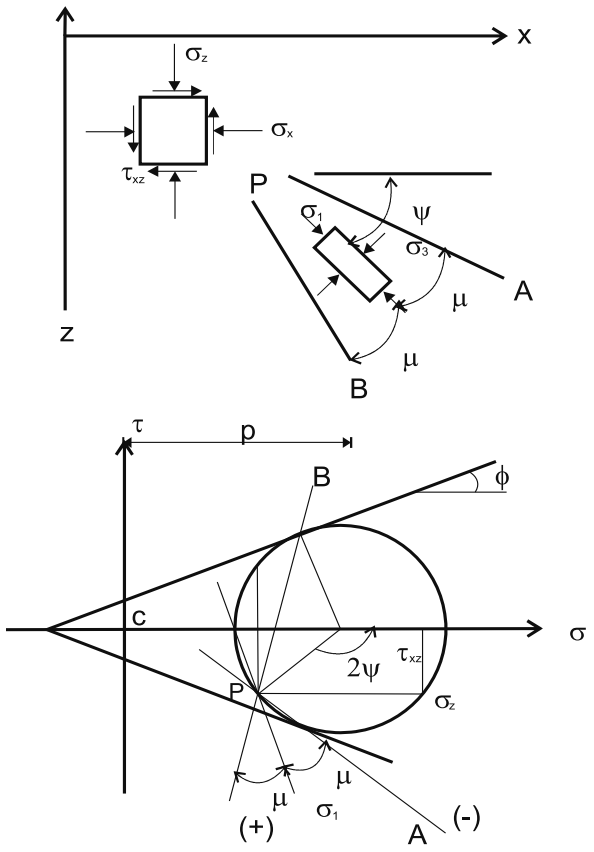

Figure 1. The orientation of the positive (σ^+) and negative (σ^-) characteristics and the Mohr's circle of stress [16].

If the body forces are zero, the equilibrium equations along the stress characteristics can be written as [9]:

$$2\left(p\tan\phi + c\right)d\psi + dp = 0 \qquad (1)$$

$$2\left(p\tan\phi + c\right)d\psi - dp = 0 \qquad (2)$$

2.1 Boundary conditions

Figure 2 shows the geometry of the problem. DE is the ground-surface boundary and has the surcharge q. β is the ground-surface angle with the horizontal axis and θ is the angle between the wall and the vertical axis. The positive signs of these angles are shown in the figure. k_h and k_v are the horizontal and vertical pseudo-static earthquake coefficients, respectively. The positive directions of the seismic accelerations are shown in the figure. To solve the problem, the boundary condition of the wall and ground surface must be calculated.

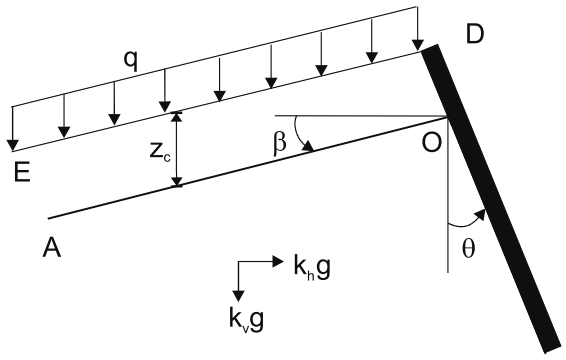

Figure 2. The geometry of the problem.

The Mohr's circles of stress along the ground surface and wall boundaries are shown in Figure 3. The normal and shear stresses on the ground surface can be written as

$$\sigma_0 = \overline{q}\cos\beta\left[\left(1-k_v\right)\cos\beta - k_h\sin\beta\right] = A_1\overline{q} \qquad (3)$$

$$\tau_0 = \overline{q}\cos\beta\left[\left(1-k_v\right)\sin\beta + k_h\cos\beta\right] = A_2\overline{q} \qquad (4)$$

where $\overline{q}$ is the equivalent surcharge (Eq. (18)) and

$$A_1 = \frac{\left(1-k_v\right)\cos\beta\cos\left(\delta+\beta\right)}{\cos\delta}$$
$$A_2 = \frac{\left(1-k_v\right)\cos\beta\sin\left(\delta+\beta\right)}{\cos\delta} \qquad (5)$$

and

$$\tan\delta = \frac{k_h}{1-k_v} \qquad (6)$$

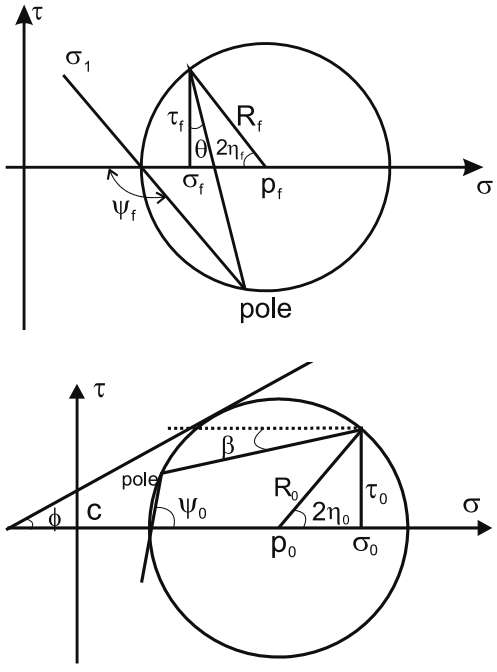

Figure 3. Mohr's circle of stress of the a) wall and b) ground surface.

The radius of the Mohr's circle on the ground surface can be written as (Figure 3b)

$$R_0 = p_0 \sin\phi + c\cos\phi = \sqrt{\left(\sigma_0 - p_0\right)^2 + {\tau_0}^2} \qquad (7)$$

From Eq. (7), the average stress on the ground surface, p_0, is

$$p_0 = \frac{\sigma_0 + c\cos\phi\sin\phi - \sqrt{\left(\sigma_0 \sin\phi + c\cos\phi\right)^2 - \left(\tau_0 \cos\phi\right)^2}}{\cos^2\phi} \qquad (8)$$

and using the Mohr's circle, we can write

$$\begin{aligned} \eta_0 &= \pi/2 + \beta - \psi_0 \\ \sigma_0 &= p_0 + \left(p_0 \sin\phi + c\cos\phi\right)\cos 2\eta_0 \\ \tau_0 &= \left(p_0 \sin\phi + c\cos\phi\right)\sin 2\eta_0 \end{aligned} \qquad (9)$$

The angle ψ_0 can be obtained from Eq. (9) as

$$\psi_0 = \frac{\pi}{2} + 0.5\left[\beta - \delta - \sin^{-1}\left(\frac{p_0 \sin\left(\delta + \beta\right)}{p_0 \sin\phi + c\cos\phi}\right)\right] \qquad (10)$$

Referring to Figure 3a, on the retaining wall boundary

$$\begin{aligned} \eta_f &= \psi_f - \pi/2 - \theta \\ \sigma_f &= p_f - \left(p_f \sin\phi + c\cos\phi\right)\cos 2\eta_f \\ \tau_f &= c_w + \sigma_f \tan\delta_w = \left(p_f \sin\phi + c\cos\phi\right)\sin 2\eta_f \end{aligned} \qquad (11)$$

The angle ψ on the wall, ψ_f, can be found from Eq. (11) as

$$\psi_f = \frac{\pi}{2} + \theta + 0.5\left[-\delta_w + \sin^{-1}\left(\frac{p_f \sin\delta_w + c_w \cos\delta_w}{p_f \sin\phi + c\cos\phi}\right)\right] \qquad (12)$$

2.2 Calculating the plastic critical depth

Since the stresses on the left- and right-hand side of point O are different, this point is a singularity point. To obtain the depth of the plastic critical depth without computing the whole network, the singularity point must be solved. If $\psi_f \geq \psi_0$, the stresses are continuous everywhere, but when $\psi_f < \psi_0$, there is a line of discontinuity in the stress field, which will be explained next. This type of discontinuity has been considered in some studies [9, 11, 17, 18]. Peng and Chen [13] stated that the solution obtained from this discontinuity is a virtual solution and does not represent reality. In this paper the discontinuity is used and the obtained results are in good agreement with other solutions.

If $\psi_f \geq \psi_0$, from Eq. (1), p_f can be found as

$$\begin{aligned} &\text{If} \quad \phi{=}0: \quad p_f = p_0 - 2c\left(\psi_f - \psi_0\right) \\ &\text{else} \quad : \quad p_f = -c\cot\phi + \left(p_0 + c\cot\phi\right)\exp\left[-2\tan\phi\left(\psi_f - \psi_0\right)\right] \end{aligned} \qquad (13)$$

But if $\psi_f < \psi_0$, a line of discontinuity exists in the problem. In this paper an approach similar to that of Lee and Herington [17] is used to solve this discontinuity. Figure 4 shows a soil element on the discontinuity line and Mohr's circle of stress for the left- and right-hand sides of this element.

Referring to Mohr's circle of stress (Figure 4), we can write

$$R_R \sin 2\left(\psi_R - \omega\right) = R_L \sin 2\left(\psi_L - \omega\right) \qquad (14)$$

$$p_R - R_R \cos 2\left(\psi_R - \omega\right) = p_L - R_L \cos 2\left(\psi_L - \omega\right) \qquad (15)$$

where ω is the angle between the discontinuity line and the horizontal axis, p_R, R_R and ψ_R are the average stress, the radius of the Mohr's circle and the angle ψ for the right-hand side of the discontinuity line, respectively. These parameters for the left-hand side of the discontinuity line are denoted by p_L, R_L and ψ_L. Using Eq. (14) and (15), ω and p_R can be obtained as

$$\omega = 0.5\left[\psi_R + \psi_L - \cos^{-1}\left(\sin\phi\cos\left(\psi_R - \psi_L\right)\right)\right] \qquad (16)$$

$$p_R = \frac{R_L \sin 2\left(\psi_L - \omega\right)}{\sin\phi \sin 2\left(\psi_R - \omega\right)} - c\cot\phi \qquad (17)$$

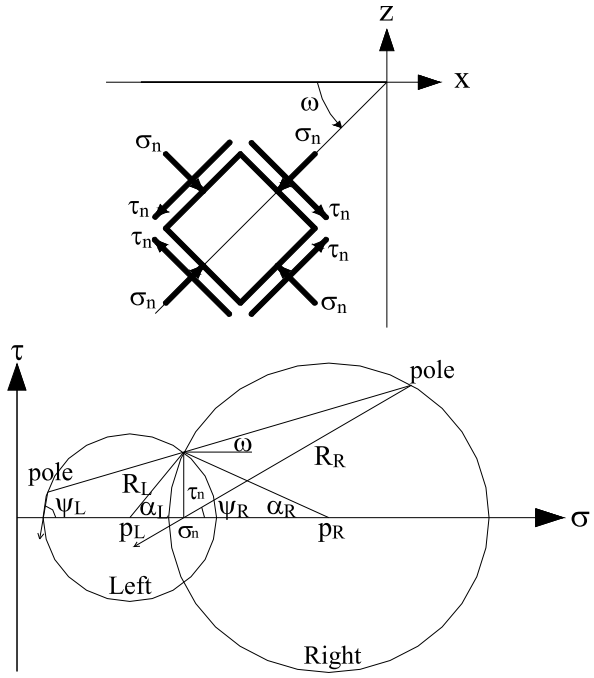

Figure 4. A soil element on the discontinuity line and Mohr's circle of stress of the element.

To calculate the plastic critical depth in active lateral earth pressure problems, an equivalent surcharge can be used [13]. This uniform equivalent surcharge on the OA boundary (Figure 2) can be written as

$$\overline{q} = q + \gamma z_c \qquad (18)$$

where z_c is the plastic critical depth and γ is the unit weight of the soil.

The equivalent surcharge $\overline{q}$ must be computed such that the normal stress on the wall is zero. When $\sigma_f = 0$, from Eq. (11) and (12) [13]

$$p_f = c\tan\phi + \frac{\sqrt{c^2 - {c_w}^2}}{\cos\phi} \qquad (19)$$

If $\psi_f \geq \psi_0$, the value of p_0 can be obtained from Eq. (13) as

$$\begin{aligned} &\text{If} \quad \phi{=}0: \quad p_0 = p_f + 2c\left(\psi_f - \psi_0\right) \\ &\text{else} \quad : \quad p_0 = -c\cot\phi + (p_f + c\cot\phi)\exp\left[2\tan\phi\left(\psi_f - \psi_0\right)\right] \end{aligned} \qquad (20)$$

and if $\psi_f < \psi_0$, using Eq. (17)

$$p_0 = -c\cot\phi + \sin 2\left(\psi_f - \omega_0\right)\frac{p_f + c\cot\phi}{\sin 2\left(\psi_0 - \omega_0\right)} \qquad (21)$$

where from Eq. (16)

$$\omega_0 = 0.5\left[\psi_f + \psi_0 - \cos^{-1}\left(\sin\phi\cos\left(\psi_f - \psi_0\right)\right)\right] \qquad (22)$$

Finally, from Eqs. (3), (4) and (7)

$$\overline{q} = \frac{A_1 p_0 + \sqrt{\left(p_0\sin\phi + c\cos\phi\right)^2\left({A_1}^2 + {A_2}^2\right) - \left(p_0 A_2\right)^2}}{{A_1}^2 + {A_2}^2} \qquad (23)$$

To calculate $\overline{q}$, first, p_f and ψ_f are calculated from Eqs. (19) and (12). Since p_0 and ψ_0 are not independent of each other, a trial-and-error procedure must be used to compute these parameters. First, an initial value is assumed for p_0, then ψ_0 is computed from Eq. (10) and based on the value of ψ_0, a new value for p_0 is obtained from Eq. (20) or (21). This procedure is repeated until the differences between the new and old values of p_0 and ψ_0 are small enough. Having p_0, the value of $\overline{q}$ can be calculated from Eq. (23) and finally z_c is obtained from Eq. (18) as

$$z_c = \frac{\overline{q} - q}{\gamma} \geq 0 \qquad (24)$$

In the static case, when β=0, the plastic critical depth can be computed without trial and error. When $\psi_f \geq \psi_0$, and for the static case, the results of this paper are the same as those of Peng and Chen [13].

3 RESULTS

Based on the algorithm described in the previous section, a computer code was prepared. In this part of the paper different parametric analyses were made for the plastic critical depth, and the results were compared to the results of the other studies.

In the static case (k_h=k_v=0) and for δ_w=c_w=θ=β=0, the solution leads to the following equation, which is the simple Rankin formula for the plastic critical depth

$$z_c = \frac{2c}{\gamma}\tan\left(\frac{\pi}{4} + \frac{\phi}{2}\right) - \frac{q}{\gamma} \qquad (25)$$

Nian and Han [4] developed the Rankin theory to calculate the seismic active lateral earth pressure. They neglected the friction angle and the adhesion of the soil-wall interface and assumed that the wall is vertical (i.e., δ_w=c_w=θ=0). Their equation for z_c is

$$z_c = \frac{2c\left(\sin\phi\left(1 - \tan\beta\tan\delta\right) + \sqrt{\left(1 - \tan\beta\tan\delta\right)^2 + 4\tan^2\delta}\right)}{\gamma\left(1 - k_v\right)\cos\phi\left(\left(1 - \tan\beta\tan\delta\right)^2 + \dfrac{4\tan^2\delta}{\cos^2\phi}\right)} \qquad (26)$$

Also, Peng [3] developed the Mononobe-Okabe theory for the seismic case by taking into account the effect of the plastic critical depth and proposed the following equation to calculate $\overline{q}$

$$\overline{q}=\frac{c\cos(\theta-\beta)\cos\phi+c_w\sin(\alpha_a+\beta)\sin(\alpha_a+\theta-\phi)}{\sqrt{k_h{}^2+(1-k_v)^2}\cos(\alpha_a+\theta)\sin(\alpha_a-\phi-\delta)\cos\beta} \quad (27)$$

where

$$\tan\alpha_a=\frac{\sin(\phi+\delta-\theta)+m_0\sin\theta\cos\theta+\sqrt{1-m_0\cos(\theta+\phi+\delta)}}{\cos(\theta-\phi-\delta)+m_0\sin^2\theta}$$
$$m_0=\frac{c_w\cos(\beta+\delta)}{(c+c_w)\cos(\theta-\beta)\cos\phi} \quad (28)$$

In addition, α_a can also be calculated using the following equations:

$$\text{if}\quad c\cos(\theta-\beta)\cos\phi+c_w\sin(\phi+\beta+\delta)\sin(\theta+\delta)>0,\quad \text{then}$$
$$\tan\alpha_a=\frac{\sin(\phi+\delta-\theta)+n_0\sin(\phi+\delta)\cos(\phi+\delta)+\sqrt{1+n_0\cos(\theta+\phi+\delta)}}{\cos(\theta-\phi-\delta)+n_0\cos^2(\phi+\delta)}$$
$$n_0=\frac{c_w\cos(\beta+\delta)}{c\cos(\theta-\beta)\cos\phi+c_w\sin(\phi+\beta+\delta)\sin(\theta+\delta)} \quad (29)$$
$$\text{if}\quad c\cos(\theta-\beta)\cos\phi+c_w\sin(\phi+\beta+\delta)\sin(\theta+\delta)=0,\quad \text{then}\ \alpha_a=\phi+\delta$$

A comparison of the results of this paper with the results of the other methods is shown in Table 2. The percentage relative errors between the results of this paper and the other methods are shown in the table as well. In the last row of the table the average percentage errors for all the cases are written. It is clear that the least and the most errors belong to Peng's limit-equilibrium method [3] (average error 3%) and Eq. (25) (average error 38%), respectively. In addition, the depths computed from the stress-characteristics method are lower than those of the other methods.

In the static case and for q=θ=0, a comparison was made between the results of this study for z_c and those of others, as shown in Figure 5. In this case the results of Eq. (25), Nian and Han [4] and Iskander et al. [5] are the same. It is clear that the results of this study are very close to Peng [3] (average difference is about 1.4%). Eq. (25) predicts smaller values of z_c (about 15% smaller) and also the results of Lin et al. [7] are about 29% smaller than the results in this paper.

To evaluate the effects of the parameters on the plastic critical depth, several parametric analyses were made. Figure 6 shows the effects of the pseudo-static horizontal (k_h) and vertical (k_v) coefficients on the plastic critical depth z_c. The horizontal axis is k_h and varies from -0.5 to 0.5. It is clear that z_c increases with an increase in k_h. When k_h is positive, its variation has more influence on increasing z_c. For example, if k_v=0, when k_h changes from 0 to -0.5, z_c decreases by about 58%, but when k_h changes from 0 to 0.5, the increase in z_c is about 93%. These differences in the negative values of k_v are less than those of the positive values.

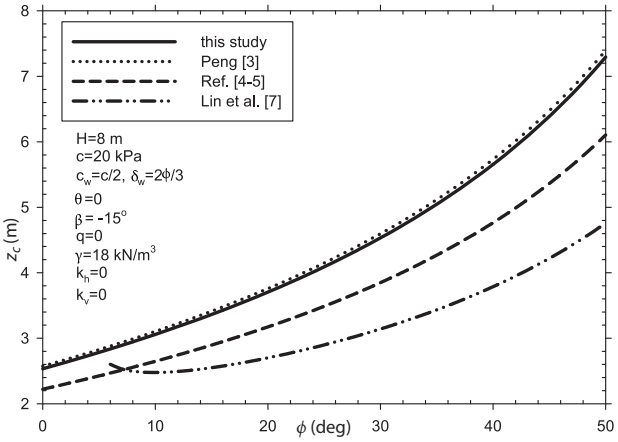

Figure 5. A comparison between the results of this study and those of others.

Table 2. Comparison of the results of this study with other methods. (θ=-10º, β=0, δ_w=ϕ/2, c_w=0.5c, k_h=-0.2, k_v=0.1, γ=18 kN/m^3).

ϕ (deg)	c (kPa)	q (kPa)	z_c (m)					Absolute relative error (%)			
			Ma et al. 2012, [6]	Eq. (25)	Nian & Han, 2013, [4]	Peng, 2012,[3]	This study	Ma et al. 2012, [6]	Eq. (25)	Nian & Han, 2013, [4]	Peng, 2012, [3]
20	0	10	0	0	0	0	0	0	0	0	0
20	10	0	1.424	1.592	1.315	1.224	1.206	15	24	8	1
20	10	10	0.904	1.032	0.759	0.668	0.651	28	37	14	3
40	10	0	1.68	2.384	1.837	1.442	1.382	18	42	25	4
40	10	10	1.168	1.832	1.281	0.886	0.826	29	55	36	7
20	20	0	2.6	3.168	2.629	2.447	2.412	7	24	8	1
20	20	10	2.072	2.624	2.074	1.892	1.857	10	29	10	2
40	20	0	3.048	4.768	3.674	2.884	2.764	9	42	25	4
40	20	10	2.52	4.208	3.118	2.328	2.208	12	48	29	5
Average error:								16	38	19	3

Also, increasing k_v leads to an increase in z_c. Similar to k_h, when k_v is positive, the variations are more rapid. The average changes in z_c for k_v= -0.5 relative to k_v=0 are about 22% and 40% in the negative and positive values of k_h, respectively. These changes for k_v=0.5 relative to k_v=0 are 39% and 144% in the negative and positive values of k_h, respectively.

The results of Peng [3] are also shown in Figure 6. It is clear that the values of results of this study are lower than those of Peng. For the selected parameters shown in the figure, the average relative errors between these two methods are 1% for the positive values of k_h and k_v and 30% for the negative values of k_h and k_v.

The effects of the soil friction angle (ϕ) and ground-surface slope angle (β) values on z_c are shown in Figure 7. It is clear that z_c increases with an increase in ϕ. The results of the analyses indicate that the soil-wall interface friction angle (δ_w) has very little influence on z_c and its effect can be ignored.

Increasing β leads to an increase in the plastic critical depth. When β changes from -30º to 30º, z_c increases by about 17%.

Figure 8 shows the influence of the soil cohesion and soil-wall interface adhesion on z_c. The horizontal axis is the soil cohesion (c) and several graphs have been plotted for different values of c_w/c. It is obvious that by increasing c, the plastic critical depth increases. Increasing c_w/c also leads to an increase in z_c, but its influence is less than that of c. For the assumed parameters indicated in the figure, the difference between the results of c_w/c=0 and c_w/c=1 for all values of c is about 30%. The change of z_c with c is linear. The slope of this

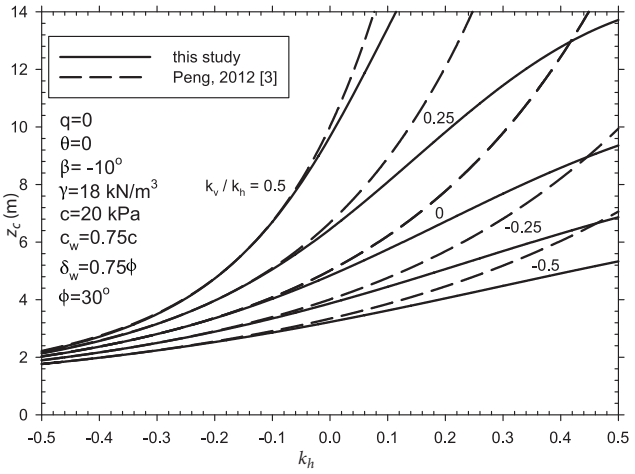

Figure 6. The effects of the k_h and k_v values on the plastic critical depth.

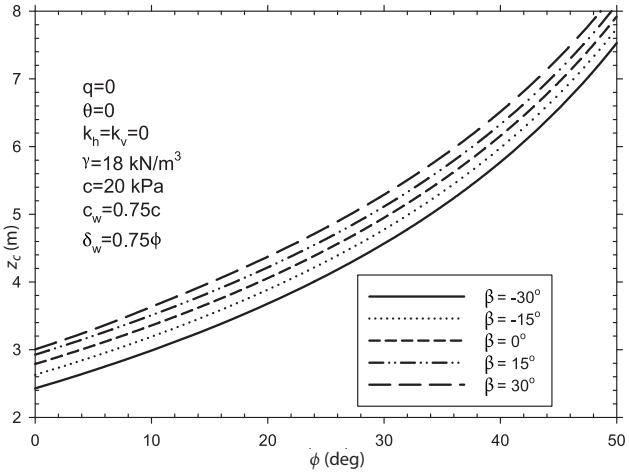

Figure 7. The effects of the ϕ and β values on the plastic critical depth.

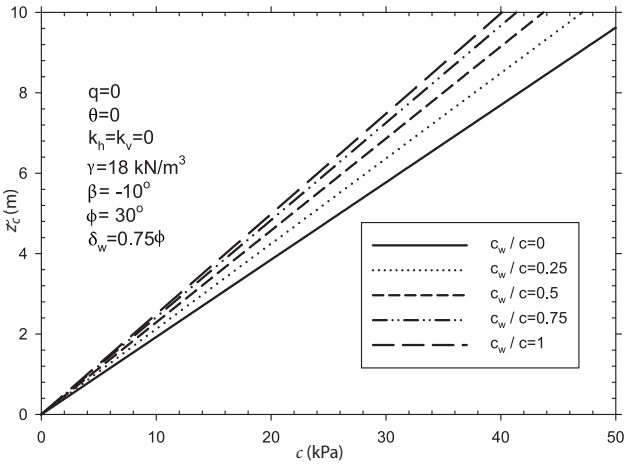

Figure 8. The effects of the c and c_w values on the plastic critical depth.

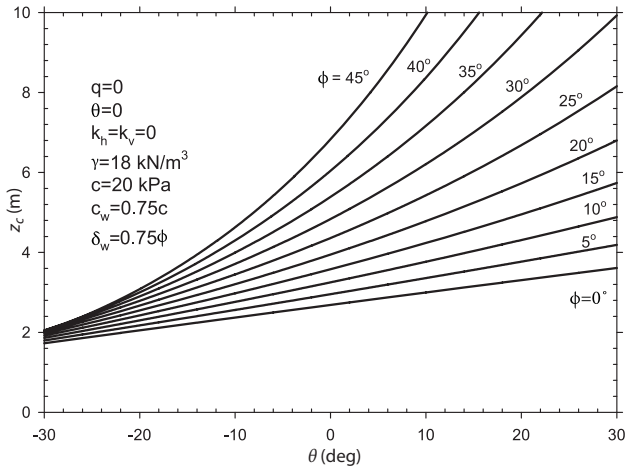

Figure 9. The effects of the θ values on the plastic critical depth.

line changes from 0.19 to 0.25 m/kPa when c_w/c changes from 0 to 1.

Figure 9 shows the influence of the wall angle (θ) on z_c. The horizontal axis shows the wall angle and changes from -30º to 30º. Different graphs have been plotted for different values of the soil friction angle. We can see that by increasing θ, the value of z_c increases. z_c varies more rapidly with θ for the larger values of ϕ. For example, when ϕ=45º, by increasing θ from -30º to 0, z_c increases by about 202%. This increase for ϕ=0, when changing θ from -30º to 0 it is about 55% and when changing θ from 0 to 30º it is about 34%.

4 CONCLUSIONS

The stress-characteristics method has been used to evaluate the plastic critical depth. The most important conclusions from this study are:

- The values of the results of the stress-characteristics method described in this paper for the plastic critical depth, z_c, are smaller than those of the pseudo--dynamic [6], modified Rankin [4] and modified Mononobe-Okabe [3] methods and are closer to the modified Mononobe-Okabe method. The method of Lin et al. [7] under predicts the plastic critical depth.
- Increasing the horizontal and vertical pseudo-static coefficients (based on their assumed directions) can increase z_c. The percentage changes relative to the static case can be more than 100%.
- The values of z_c increase with an increase in the soil friction angle, but the soil-wall interface friction angle has very little influence on z_c and can be ignored.
- For the assumed direction of the ground-surface angle β, by increasing it, z_c increases. For the sample parameters selected in this paper, by changing β from -30º to 30º, the average increase in z_c is about 17%.
- The cohesion of the soil (c) has a considerable effect on z_c. The variation of z_c with c is linear. The slope of this line increases with an increase in c_w/c.
- Increasing the wall angle (for the assumed direction of this study) leads to an increase in z_c. This effect is greater for larger values of ϕ. The influence of θ on z_c is more than that of β.

Acknowledgements

The author would like to thank the reviewer for very valuable comments and suggestions that were helpful in developing the paper.

REFERENCES

[1] Shukla, S.K., Gupta, S.K., Sivakugan, N. 2009. Active earth pressure on retaining wall for c-ϕ soil backfill under seismic loading condition, Journal of Geotechnical and Geoenvironmental Engineering 135, 5, 690-696.

[2] Peng, M.X. 2010. Analytical solution of plastic critical depth for active earth pressure on retaining wall (in Chinese), Rock and Soil Mechanics 13, 10, 3179-3183.

[3] Peng, M.X. 2012. Coulomb's solution to seismic active earth pressure on retaining walls, Chinese Journal of Rock Mechanics and Engineering 31, 3, 640-648.

[4] Nian, T., Han, J. 2013. Analytical solution for Rankine's seismic active earth pressure in c-ϕ soil with infinite slope, Journal of Geotechnical and Geoenvironmental Engineering 139, 9, 1611-1616.

[5] Iskander, M., Chen, Z., Omidvar, M., Guzman, I., Elsherif, O. 2013. Active static and seismic earth pressure for c–ϕ soils, Soils and Foundations 53, 5, 639-652.

[6] Ma, S.J., Wang, K.H., Wu, W.B. 2012. Pseudo-dynamic active earth pressure behind retaining wall for cohesive soil backfill, Journal of Central South University 19, 11, 3298-3304.

[7] Lin, Y.L., Leng, W.M., Yang, G.L., Zhao, L.H., Li, L., Yang, J.S. 2015. Seismic active earth pressure of cohesive-frictional soil on retaining wall based on a slice analysis method, Soil Dynamics and Earthquake Engineering 70, 133-147.

[8] Sokolovskii, V.V. 1960. Statics of soil media, London, UK: Butterworth.

[9] Sokolovskii, V.V. 1965. Statics of granular media, Oxford, UK: Pergamon Press.

[10] Reece, A., Hettiaratchi, D. 1989. A slip-line method for estimating passive earth pressure, Journal of Agricultural Engineering Research 42, 1, 27-41.

[11] Kumar, J., Chitikela, S. 2002. Seismic passive earth pressure coefficients using the method of characteristics, Canadian Geotechnical Journal 39, 2, 463-471.

[12] Cheng, Y. 2003. Seismic lateral earth pressure coefficients for c-ϕ soils by slip line method, Computers and Geotechnics 30, 8, 661-670.

[13] Peng, M.X., Chen, J. 2013. Slip-line solution to active earth pressure on retaining walls, Geotechnique 63, 12, 1008-1019.

[14] Jahanandish, M., Keshavarz, A. 2005. Seismic bearing capacity of foundations on reinforced soil slopes, Geotextiles and Geomembranes 23, 1, 1-25.

[15] Keshavarz, A., Jahanandish, M., Ghahramani, A. 2011. Seismic bearing capacity analysis of rein-

forced soils by the method of stress characteristics, Iranian Journal of Science and Technology, Transaction of Civil Engineering 35, C2, 185-197.

[16] Anvar, S.A., Ghahramani, A. 1997. Equilibrium equations on zero extension lines and their application to soil engineering, Iranian Journal of Science and Technology, Transaction B-Engineering 21, 1, 11-34.

[17] Lee, I.K., Herington, J.R. 1972. A theoretical study of the pressures acting on a rigid wall by a sloping earth or rock fill, Geotechnique 22, 1, 1-26.

[18] Liu, F.Q., Wang, J. H. 2008. A generalized slip line solution to the active earth pressure on circular retaining walls, Computers and Geotechnics 35, 2, 155-164.